

## RESEARCH ARTICLE



## STRUCTURE AND MORPHOLOGICAL STUDIES OF RARE EARTH DOPED NICKEL-MAGNESIUM NANOFERRITES SYNTHESIZED BY SOL-GEL METHOD

V V J GOPALA KRISHNA<sup>1</sup>, M.RAMA REDDY<sup>2</sup>

<sup>1</sup>Senior Lecturer in chemistry, Mrs A V N College, Visakhapatnam, Andhra Pradesh

<sup>2</sup> SG Lecturer in chemistry, G.B.R College, Anaparthi, E.G. District., Andhra Pradesh

Article Received: 03/01/2014

Article Revised: 20/1/2014

Article Accepted: 28/02/2014



### ABSTRACT

Samarium ( $\text{Sm}^{3+}$ ) doping Nickel-Magnesium nano spinel ferrite ( $\text{Sm}_x, \text{Ni}_{0.2}, \text{Mg}_{0.2}, \text{Fe}_2\text{O}_4$ , (where  $x = 0.00, 0.02, 0.04$ ) compounds developed via sol-gel method. The samples thus obtained were analysed for their structural, morphological magnetic properties as a function of increasing  $\text{Sm}^{3+}$  content. Nickel ferrite being one of the most important inverse spinel ferrite has a wide range of applications especially as microwave devices. Samarium, a rare earth metal, having an electronic configuration  $4f6 6s2$  is used as a dopant along with nickel ferrite and the consequent modifications in the properties are characterized accordingly. The structural characterizations of all the prepared samples were done using XRD and FTIR. Synthesis of materials is confirmed using XRD from the report of single phase polycrystalline ferrite material. FT-IR of the  $\text{Sm}^{3+}$  doped ferrites analyzed in the range of  $4000-400\text{cm}^{-1}$ . The absorption bands ' $\nu_1$ ' and ' $\nu_2$ ' are assigned to the intrinsic stretching vibrations of tetrahedral complexes and octahedral complexes respectively. Crystallinity and the crystallite size are observed to increase with the concentration of samarium. The surface morphology and particle size of a typical sample were determined using SEM and TEM respectively. Surface morphology studied by SEM and particle size determined by TEM.

Keywords: Ni-Mg nanoferrites, Surface morphology, XRD, FTIR, TEM, Magnetic Properties

©KY PUBLICATIONS

### 1.0 Introduction

Nanocrystalline spinel ferrites are technologically important because of their wide applications, and it is believed that the production of ferrites will increase year by year as their applications become more and more diverse. Doping ferrite nanocrystals with various metals, such as chromium, copper, manganese, and zinc are usually used to improve some of their electric or magnetic properties<sup>1</sup>. Nickel ferrite and nickel based mixed ferrite nanoparticles are of technical importance due to numerous applications in electronics<sup>2</sup>. These are promising materials for use in telecommunication equipment, computer peripherals, and other electronic

and microwave devices. The substitution of the rare earth ions into the inverse spinel lattice induces a strain due to which the electrical and magnetic properties are significantly modified<sup>3</sup>. Rashad et al (2011)<sup>4</sup> reported a change in the magnetic properties of samarium doped cobalt ferrite nanoparticles synthesized by the citrate precursor route. The results reported a decrease in the value of the saturation magnetization and coercivity upon the addition of Sm<sup>3+</sup> ions. Tahar et al (2007)<sup>5</sup> investigated the effect of gadolinium and samarium doping on the magnetic properties of cobalt ferrite nanoparticles synthesized using forced hydrolysis in polyol and concluded that there was a slight increase in the crystallite size during the rare earth substitution. In this paper we report the effects of Sm<sup>3+</sup> substitution on the structural and magnetic properties of nickel ferrite nanoparticles synthesized by the sol-gel route.

Magnetic properties of ferrites depend on their chemical composition, preparation method, sintering time and temperature<sup>6</sup>. The sol-gel method is used for the synthesis of Nickel substituted cobalt ferrite nanoparticles. The result proves that with increase in nickel content magnetic saturation decreases<sup>7</sup>. Infrared spectroscopy (IR) is one of the most powerful techniques, which offers possibility of chemical identification. One of the advantages of IR over other methods for structural analysis is that, it provides useful information about the structure of a molecule rapidly and also without cumbersome evaluation methods. The technique is based upon the simple fact that a chemical substance shows marked selective adsorption in the infrared region. Various bands obtained in IR spectra are corresponding to the characteristic functional groups and bonds present in the chemical substance. The absorption bands in the IR spectra split on the basis of different cations present on tetrahedral (A) and octahedral [B] sites of spinel ferrites<sup>8</sup>. Nickel ferrites are stable, relatively inexpensive and easily manufactured and have wide applications in electronics and communication industries owing to their interesting magnetic and electrical properties. In this work, we study effects of Sm<sup>3+</sup> ion in substitutions on Mg/Ni ferrite nanocrystals synthesized through the sol-gel method. Specifically, we characterize structural and magnetic properties of the doped samples at room temperature.

## 2.0 Experimental

### 2.1 Material and Method

All chemicals and solvents were AR grade or better purchased from Merck Co.Pvt Ltd and Sd. fine chemical used without any further purification. The stoichiometric amounts of metal nitrates (Ni, Mg, and Sm) Citric acid - (C<sub>6</sub>H<sub>8</sub>O<sub>7</sub>.H<sub>2</sub>O) used as starting materials for the synthesis.

### 2.2 Synthesis of nanoparticles

Metal nitrates in required proportions were dissolved in a minimum quantity of distilled water and mixed together. Aqueous solution of Citric acid was then added to the mixed metal nitrate solution (with and without Samarium nitrate). Ammonia solution was then added with constant stirring by maintaining the neutral pH (7.0). The solutions were heated at 90°C under continuously stirring to remove the excess of the solvent. By raising the temperature up to 200°C lead the ignition of gel. The dried gel burnt completely in a self-propagating combustion manner to form powder like substance. The burnt powder was ground in Agate Mortar and Pestle to get a fine Ferrite powder. Finally the burnt powder was calcined in air at 700°C temperature for 2 hours and cooled to room temperature.

### 2.3 Characterization

#### 2.3.1 X-ray Diffraction

The XRD analysis on the prepared samples was made using a SCINTAG X'TRA AA85516 (Thermo ARL) X-ray diffractometer equipped with a Peltier cooled Si solid detector. Monochromatized Cu K<sub>α</sub> (λ = 1.5405 Å) was used as the radiation. Diffraction patterns were collected at 45 kV–40 mA, at 0.02°C step and count time of 0.400 sec over a range of 10.00–80.0 (2θ), at a step scan rate of 3.00 min<sup>-1</sup> and the crystallite size (D) is calculated from X-ray line broadening of the (311) diffraction peak using the well-known Debye-Scherrer's formula<sup>9</sup>:

$$D = \frac{0.9\lambda}{\beta \cos\theta}$$

where  $\beta$  is the full-width at half-maxima of the strongest intensity diffraction peak (311),  $\lambda$  the wavelength of the radiation, and  $\theta$  the angle of the strongest characteristic peak.

X-ray density ( $\rho_x$ ) was calculated using the following equation:

$$\rho_x = \frac{8M}{Na^3}$$

where  $M$  is the molecular weight (gm),  $N$  Avogadro's number (per mol) and  $a$  the lattice parameter in angstrom.

The value of lattice parameter  $a$  determined from the high intense peak (311) of XRD pattern using the following equation<sup>10</sup> and values are given in Table 1.

$$a = \frac{d_{hkl}}{(\sqrt{h^2 + k^2 + l^2})}$$

where  $a$  is lattice constant  $d_{hkl}$  is inter-planar distance for  $hkl$  plane.

### 2.3.2 FTIR Spectroscopic Analysis

The adsorbents are examined using Fourier Transform Infrared spectroscopy (FTIR). The sample discs were prepared by mixing of 1 mg of powdered carbon with 500 mg of KBr (Merck-spectroscopy quality) in an agate mortar, then pressing the resulting mixture successively under a pressure of 5 tones/ cm<sup>2</sup> for about 5 min., and at 10 tones/ cm<sup>2</sup> for 5 min., under vacuum. The spectra were measured from 4000 to 400 cm<sup>-1</sup> on a JASCO-FTIR-5300 model.

### 2.3.3 SEM-EDX analysis

The surfaces of the powder carbonaceous materials have been stubbed using the double-sided adhesive carbon tape. Samples are coated with the help of platinum coater [JOEL Auto fine coater model, JFC -1600 auto fine coater, Coating time is 120 sec with 20mA] and deposited with a thin layer of platinum on the sample. The microphotographs of these samples were recorded using SEM JEOL model, JSM-5600 equipped with EDX Analyzer, an accelerating voltage of 5 kV, at high vacuum mode. The maximum magnification possible in the equipment is 3,00,000 times with a resolution of 3 nm, typically setting at various magnifications for all the samples of study.

### 2.3.4 TEM analysis

The ferrite sample was first sonicated (Vibronics VS 80) for 5 minutes. Ferrites were loaded on carbon coated copper grids, and solvent was allowed to evaporate under Infra light for 30 minutes. TEM measurements were performed on Phillips model CM 20 instrument, operated at an accelerating voltage at 200 kV.

Hysteresis Tracer was employed to study the magnetic properties of the samples in the field of 10 kOe at room temperature.

## 3. RESULTS & DISCUSSION

In general, the sol-gel process involves several successive stages: (a) formation of sol which represents a colloidal suspension containing small particles with a diameter less than 1000 nm dispersed in a continuous liquid medium, (b) the gelation of the sol to give a three-dimensional M-O-M/M-OH-M network whose pores are filled with solvent molecules (wet gel), (c) the ageing of the resulting wet gel process known as syneresis, (d) the elimination of the solvent from the gel's pore (drying)

**3.1 XRD analysis:** A series of three samples with general formula (Sm<sub>x</sub>, Ni<sub>0.2</sub>, Mg<sub>0.2</sub>, Fe<sub>2</sub>O<sub>4</sub>, (where x = 0.00, 0.02, 0.04) were prepared by the sol-gel technique. XRD analysis confirmed the formation of single phase FCC spinel structure. Samarium on (Sm<sup>3+</sup>) doping has resulted in an increase in lattice parameter and increase in particle size of Ni-Mg ferrite. The increase in lattice parameter due to increased doping (x > 0.04) indicated a possible cationic redistribution.

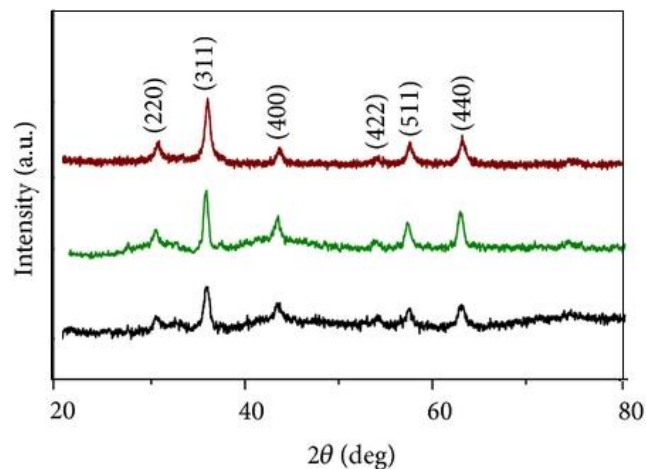


Figure 1: XRD Spectra of Sm-Ni-Mg Spinel nanoferrites

The lattice parameter, average crystallite size, and lattice strain obtained for all the samples are given in Table 1.

Table 1: Table 1: Effect of  $\text{Sm}^{3+}$  substitution on the lattice parameter, crystallite size, X-ray density, and lattice strain of Sm-Ni-Mg nanocrystalline ferrites

Sm content	Lattice parameter ( $\text{\AA}$ )	Crystallite size (nm)	X-ray density ( $\text{g cm}^{-3}$ )	Lattice strain %
0	8.567	$34.24 \pm 2.5$	5.365	-0.197
0.02	8.572	$32.08 \pm 2.5$	5.464	0.198
0.04	8.579	$31.37 \pm 2.5$	5.558	0.067

It can be seen from Table 1 that the average crystallite size of the samples shows an increasing trend with the increase in the concentration of samarium. Various researchers have reported increase in crystallite size of ferrite nanoparticles by the substitution of rare earth ions<sup>11</sup>. The increase in the crystallite size can be considered as a good indication of improved crystallinity and great chemical homogeneity<sup>12</sup>. The low value of lattice strain obtained for the samarium-doped samples also indicates the improved crystallinity. An increase in lattice parameter with increase in  $\text{Sm}^{3+}$  ion content is expected because of the large ionic radius of  $\text{Sm}^{3+}$  (0.0964 nm) compared to that of  $\text{Fe}^{3+}$  (0.0645 nm).  $\text{Sm}^{3+}$  ions are expected to enter into the octahedral sites in place of  $\text{Fe}^{3+}$  ions which could result in an internal stress to make the lattice distorted and an expansion of unit cell.

### 3.2 FT IR Analysis

FTIR spectra of the investigated samples in the wave number range  $850\text{--}400\text{ cm}^{-1}$  are shown in Figure 2. The prominent bands  $\nu_1$  and  $\nu_2$  are present in all the samples. The vibrational frequencies of the IR bands are in agreement with the reported values<sup>13</sup>. It can be seen from Figure 5 that the values of  $\nu_1$  and  $\nu_2$  shift to lower-frequency side with increasing samarium content. Also a slight broadening of the absorption band is also noticed with increase in samarium concentration. This may be attributed to the substitution of  $\text{Fe}^{3+}$  ions by  $\text{Sm}^{3+}$  ions. In the wave number range of  $430\text{--}600\text{ cm}^{-1}$ , two main broad metal–oxygen bands are seen in the infrared spectra of all spinels, especially ferrites. The higher one ( $\nu_1$ ) generally observed in the range  $550\text{--}600\text{ cm}^{-1}$ , is caused by the stretching vibrations of the tetrahedral metal–oxygen bond. The lowest band ( $\nu_2$ ) usually observed in the range  $430\text{--}440\text{ cm}^{-1}$ , is caused by the metal–oxygen vibrations in the octahedral sites. This difference in the spectral positions is expected because of the difference in the  $\text{Fe}^{3+}\text{--O}^{2-}$  distance for the octahedral and tetrahedral compounds. This is confirmed from Fourier Transform Infrared Spectroscopy (FTIR) that the structure remains cubic spinel after  $\text{Sm}^{3+}$  ion substitution in Ni-Mg nano ferrites.

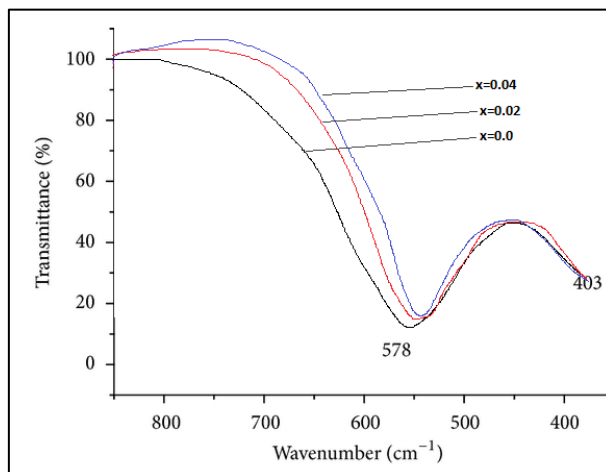


Figure 2: FTIR spectra of the nanoferrite samples ( $\text{Sm}_x, \text{Ni}_{0.2}, \text{Mg}_{0.2}, \text{Fe}_2\text{O}_4$ , (where  $x = 0.00, 0.02, \text{ and } 0.04$ )

**3.3 SEM analysis:** The SEM images of Sm-Ni-Mg nanocrystalline ferrites by sol-gel method as shown in figure-3. The SEM image of the prepared  $\text{Sm}_{0.04}, \text{Ni}_{0.2}, \text{Mg}_{0.2}, \text{Fe}_2\text{O}_4$  sample is composed of nanocrystals and shows the distribution of nanoparticles.

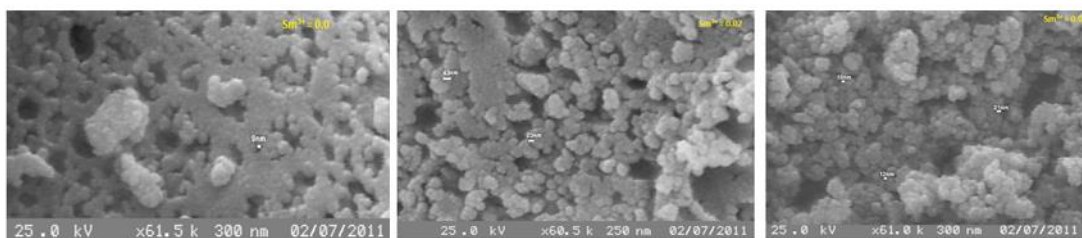


Figure 3: SEM image of the nanoferrite samples ( $\text{Sm}_x, \text{Ni}_{0.2}, \text{Mg}_{0.2}, \text{Fe}_2\text{O}_4$ , (where  $x = 0.00, 0.02, \text{ and } 0.04$ )

**3.4 EDAX analysis:** The typical EDAX spectra taken from the ferrite grain and grain boundary of a typical sample  $\text{Sm}_{0.04}, \text{Ni}_{0.2}, \text{Mg}_{0.2}, \text{Fe}_2\text{O}_4$  to know the chemical constituents present in the materials and it reveals that the ferrite grain contain amount of  $\text{Sm}^{3+}$  supporting indirectly the entering of  $\text{Sm}^{3+}$  ions into the sub lattice of ferrites. The EDAX spectrum (Figure 4a&4b) shows the content of  $\text{Sm}^{3+}$  is less than that of its normal composition due to segregation of  $\text{Sm}^{3+}$  ions into the grain boundaries and evaporation at high temperature. Also it is found that grain sizes of the samples increases with increasing in doping of  $\text{Sm}^{3+}$  ions because more cations vacancies, closed pores exist and grain boundary movement when large amount of  $\text{Sm}^{3+}$  ions exist in the samples<sup>14</sup>.

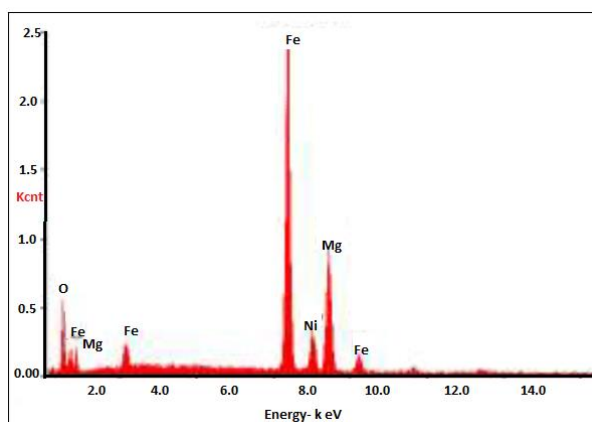


Figure 4a EDAX spectrum of  $\text{Sm}_{0.0}, \text{Ni}_{0.2}, \text{Mg}_{0.2}, \text{Fe}_2\text{O}_4$  sample

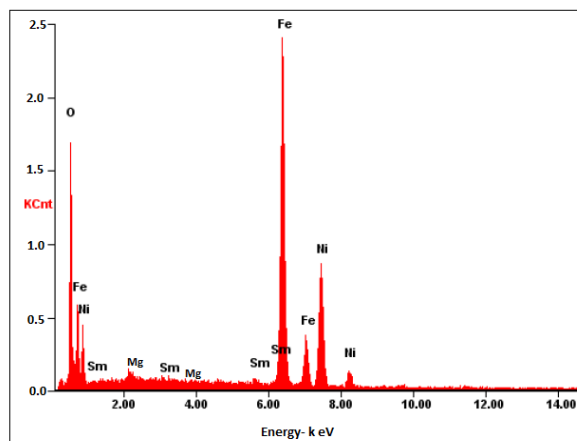


Figure 4b EDAX spectrum of  $\text{Sm}_{0.04}, \text{Ni}_{0.2}, \text{Mg}_{0.2}, \text{Fe}_2\text{O}_4$  sample

The composition of the sample was verified using the EDAX spectrum and is as indicated in Figure 3b. The spectrum shows the presence of Sm, Ni, Fe and Mg in the sample and no other appreciable impurities were detected, which indicated the purity of the sample. Moreover the ratio of the detected elements matched the chemical formula for the respective compositions. Hence the sol-gel method has indeed produced fairly good ferrites

**3.4 TEM analysis:** The particle size was estimated using TEM analysis. The reduction in particle size with rare earth doping is evident from TEM images<sup>15</sup>. Mean particle size from TEM image is in good agreement with the crystallite size measured from X-ray line (311) broadening using Scherrer's formula. Figure 5 shows Transmission Electron Micrograph of  $\text{Sm}_{0.04}, \text{Ni}_{0.2}, \text{Mg}_{0.2}, \text{Fe}_2\text{O}_4$  sample. Size of the particles obtained from TEM analysis ( $32 \pm 3 \text{ nm}$ ) is in reasonable agreement with that obtained from XRD analysis. The most of nanoparticles are in spherical shape and agglomerated due to the tendency of nanoparticles.

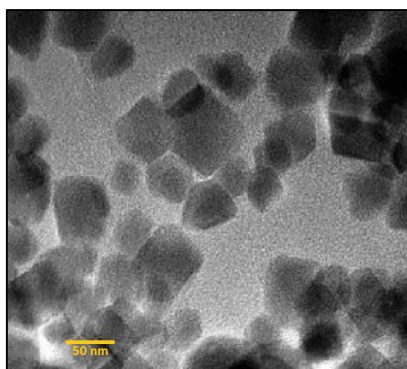


Figure 5: Transmission Electron Micrograph of  $\text{Sm}_{0.04}, \text{Ni}_{0.2}, \text{Mg}_{0.2}, \text{Fe}_2\text{O}_4$  sample

### 3.5 Magnetic properties

The magnetic parameters of prepared nano ferrite samples were calculated by using a vibrating sample magnetometer (VSM) in the range 5000 Oe, where the samples displayed the magnetic behaviour. The hysteresis loops (figure 6) were plotted from the VSM measurements, from which the saturation magnetisation values for the different compositions  $\text{Sm}_x, \text{Ni}_{0.2}, \text{Mg}_{0.2}, \text{Fe}_2\text{O}_4$  ( $x=0.0, 0.02, \& 0.04$ ) were calculated and represented graphically in Figure 6 and tabulated in table 2. The variation of saturation magnetisation with composition is as shown the figure 6 and figure 7, it was evident from the hysteresis loops that the sample does not saturate completely for values ( $x= 0.0, 0.02, 0.04$ ). From the result it is clear that the saturation magnetization decreases with the substitution of  $\text{Sm}^{3+}$ . This decrease can be explained based on the site occupancy of the cations and also the modification in the exchange effects caused by substituting  $\text{Sm}^{3+}$ . The  $\text{Fe}^{3+}$  ions occupying the 'B' sites in the inverse spinal lattice are the main contributors of the magnetic properties.  $\text{Sm}^{3+}$  paramagnetic in nature due to no unpaired electrons. There is a significant decrease in the

coercivity with the substitution of  $La^{3+}$ . This theory states that the factors such as micro strain, magneto crystalline anisotropy, magnetic particle morphology, magnetic domain size and size distribution influence the coercivity<sup>11</sup>.

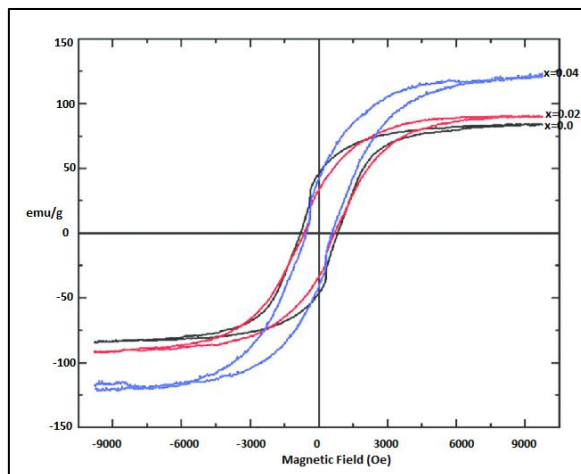


Figure 5: Hysteresis loops of Ni-Mg ferrite for various  $Sm^{3+}$  concentrations

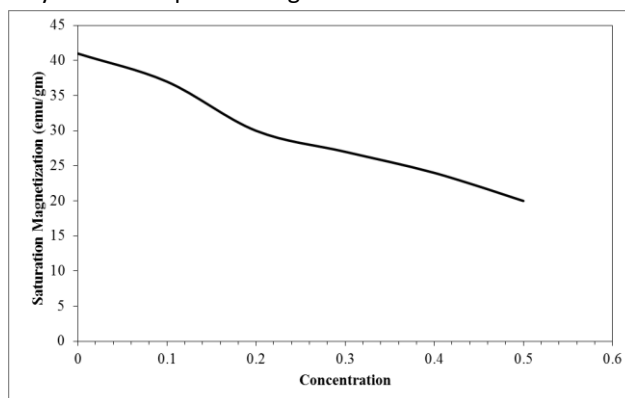


Figure 6: Plot of Magnetization Vs Concentration

Table 2: Magnetic Properties of Spinel Ferrites

Concentration of $Sm^{3+}$ ion	Magnetization (emu/g)	Coercivity (Oe)	Retentivity (emu)
0.0	21.8471	14025.21	17.264
0.02	20.6487	17245.34	16.257
0.04	18.9842	16824.57	16.128

#### 4.0 Conclusion

Samarium ion doped ( $Sm_x Ni_{0.2} Mg_{0.2} Fe_2O_4$ , (where  $x = 0.00, 0.02, 0.04$ ) nanoferrites have been successfully synthesized using sol-gel method. The formation of the ferrite powders has been confirmed by XRD, EDAX, SEM and TEM. The XRD pattern shows that nanoparticles increases with the increase in  $Sm^{3+}$  content and lattice parameter is ranging between 8.567 to 8.579Å and average particle size ranging between 32 to 35nm which will give great effect on it electric properties. It is also observed that the most of nanoparticles are in cubical shape and agglomerated due to the tendency of nanoparticles. For three samples, 'S' like shape hysteresis curve was observed. Magnetic parameters decrease with increasing  $Sm^{3+}$  substitution. The steady increase in the  $Sm^{3+}$  concentration carried about a decrease in the crystallite size tailed by a decrease in the saturation magnetisation

---

**References**

- [1]. S. Singhal, K. Chandra, Cation distribution and magnetic properties in chromium-substituted nickel ferrites prepared using aerosol route, *J. Solid. State. Chem.* 180 (2007) 296–300.
  - [2]. Khedr Mohammed Hamdy, *J. Anal. Appl. Pyrolysis* 73 (2005) 123.
  - [3]. K. K. Bharathi, J. A. Chelvane and G. Markandeyulu, "Magnetolectric properties of Gd and Nd – doped Nickel ferrite", *Journal of Magnetism and Magnetic Materials*, vol. 321, pp. 3677 – 3680, 2009
  - [4]. M. M. Rashad, R. M. Mohamed and H. El-Shall, "Magnetic properties of nanocrystalline Sm – substituted CoFe<sub>2</sub>O<sub>4</sub> synthesized by citrate precursor method", *Journal of Material Processing Technology*, vol. 198, pp. 139 – 146, 2011
  - [5]. L. B. Tahar, L.S. Smiri, M. Artus, A. –L. Joudrier, F. Herbst, M.J. Vaulay, F. Fievet, and S. Ammar, "Characterization and magnetic properties of Sm – and Gd- substituted CoFe<sub>2</sub>O<sub>4</sub> nanoparticles prepared by forced hydrolysis in polyol", *Material Research Bulletin*, vol. 42, pp. 1888 – 1896, 2007
  - [6]. A. Goldman, *Modern Ferrite Technology*, 2nd Ed., Springer, Pittsburg, 2006.
  - [7]. H.E. Zhang, B.F. Zhang, G.F. Wang, X.H. Dong, Y. Gao, The structure and magnetic properties of Ni<sub>1-x</sub>Zn<sub>x</sub>Fe<sub>2</sub>O<sub>4</sub> ferrite nanoparticles prepared by sol-gel auto-combustion, *J. Magn. Magn. Mater.* 312 (2007) 126-130
  - [8]. S. Suder, B.K. Srivastava, A. Krisnamurty, *Ind. J. Pure Appl. Phys.* 42 (2004) 366
  - [9]. P. Scherrer, *Göttinger Nachrichten Gesell.*, Vol. 2, 1918, p 98
  - [10]. Krishna, K.R., Ravinder, D., Kumar, K.V. and Lincon, C.A. (2012) Synthesis, XRD & SEM Studies of Zinc Substitution in Nickel Ferrites by Citrate Gel Technique. *World Journal of Condensed Matter Physics*, 2, 153-159
  - [11]. J. Peng, M. Hojamberdiev, Y. Xu, B. Cao, J. Wang, and H. Wu, "Hydrothermal synthesis and magnetic properties of gadolinium-doped CoFe<sub>2</sub>O<sub>4</sub> nanoparticles," *Journal of Magnetism and Magnetic Materials*, vol. 323, no. 1, pp. 133–138, 2011
  - [12]. Sheena Xavier, Smitha Thankachan, Binu P. Jacob, and E. M. Mohammed, "Effect of Samarium Substitution on the Structural and Magnetic Properties of Nanocrystalline Cobalt Ferrite," *Journal of Nanoscience*, vol. 2013, Article ID 524380, 7 pages, 2013
  - [13]. K. B. Modi, M. K. Rangolia, M. C. Chhantbar, and H. H. Joshi, "Study of infrared spectroscopy and elastic properties of fine and coarse grained nickel-cadmium ferrites," *Journal of Materials Science*, vol. 41, no. 22, pp. 7308–7318, 2006
  - [14]. B. P. Jacob, S. Thankachan, S. Xavier, and E. M. Mohammed, "Effect of Gd<sup>3+</sup> doping on the structural and magnetic properties of nanocrystalline Ni–Cd mixed ferrite," *Physica Scripta*, vol. 84, no. 4, Article ID 045702, 2011
  - [15]. Sattar, A.A., El-sayed, H.M., El-shokrofy, K.M. and El-tabey, (2005) Improvement of the Magnetic Properties of Mn-Ni-Zn Ferrite by the Non-magnetic Al<sup>3+</sup>-Ion Substitution, *Journal of Applied Sciences*, 5, 2005, 162-168.
-